Palmiter, R. E. (1975) *Cell (Cambridge, Mass.)* *4*, 189-197.
Perler, F., Efstradiatis, A., Lomedico, P., Gilbert, W., Kolodner, R., & Dodgson, J. (1980) *Cell (Cambridge, Mass.)* *20*, 555-566.
Pribnow, D. (1975) *Proc. Natl. Acad. Sci. U.S.A.* *72*, 784-788.
Proudfoot, N. J., & Brownlee, G. G. (1976) *Nature (London)* *263*, 211-214.
Robertson, M. A., Staden, R., Tanaka, Y., Catterall, J. F., O'Malley, B. W., & Brownlee, G. G. (1979) *Nature (London)* *278*, 370-372.
Rogers, J., & Wall, R. (1980) *Proc. Natl. Acad. Sci. U.S.A.* *77*, 1877-1879.
Roop, D. R., Nordstrom, J. L., Tsai, S. Y., Tsai, M.-J., & O'Malley, B. W. (1978) *Cell (Cambridge, Mass.)* *15*, 671-685.
Sanger, F., & Coulson, A. R. (1978) *FEBS Lett.* *87*, 107-110.
Schaffner, W., Kunz, G., Daetwyler, H., Telford, J., Smith, H. O., & Birnstiel, M. L. (1978) *Cell (Cambridge, Mass.)* *14*, 655-671.
Schroeder, H. W., Liarakos, C. D., Gupta, R. C., Randerath, K., & O'Malley, B. W. (1979) *Biochemistry* *18*, 5798-5808.
Staden, R. (1977) *Nucleic Acids Res.* *4*, 4037-4051.
Sullivan, D., Palacios, R., Stavnezer, J., Taylor, J. M., Faras, A. J., Kiely, M. L., Summers, N. M., Bishop, J. M., & Schimke, R. T. (1973) *J. Biol. Chem.* *248*, 7530-7539.
Sures, I., Lowry, J., & Kedas, L. H. (1978) *Cell (Cambridge, Mass.)* *15*, 1033-1044.
Talkington, C. A., Nishioka, Y., & Leder, P. (1980) *Proc. Natl. Acad. Sci. U.S.A.* *77*, 7132-7136.
Tsai, M. J., Ting, A., Nordstrom, J., Zimmer, W., & O'Malley, B. W. (1980) *Cell (Cambridge, Mass.)* *22*, 219-230.
Tsai, S., Tsai, M.-J., & O'Malley, B. W. (1981) *Proc. Natl. Acad. Sci. U.S.A.* *78*, 879-883.
Tsujimoto, Y., & Suzuki, Y. (1979) *Cell (Cambridge, Mass.)* *16*, 425-436.
Van den Berg, J., Van Oogen, A., Mantei, N., Schambock, A., Grosveld, G., Flavell, R. A., & Weissmann, C. (1978) *Nature (London)* *276*, 37-44.
Wasylyk, B., Kedinger, C., Corden, J., Brison, O. and Chambon, P. (1980) *Nature (London)* *285*, 367-373.
Weil, P. A., Luse, D. S., Segall, J., & Roeder, R. G. (1979) *Cell (Cambridge, Mass.)* *18*, 469-484.
Woo, S. L. C., & O'Malley, B. W. (1975) *Life Sci.* *7*, 1039-1048.
Woo, S. L. C., Dugaiczyk, A., Tsai, M.-J., Lai, E. C., Catterall, J. F., & O'Malley, B. W. (1978) *Proc. Natl. Acad. Sci. U.S.A.* *75*, 6988-3692.
Ziff, E. B., & Evans, R. M. (1978) *Cell (Cambridge, Mass.)* *15*, 1463-1475.

Structure of Ferric Pseudobactin, a Siderophore from a Plant Growth Promoting *Pseudomonas*†

Martin Teintze, M. B. Hossain, C. L. Barnes, John Leong,* and Dick van der Helm*

ABSTRACT: Both plant growth promoting *Pseudomonas* B10 and its yellow-green, fluorescent iron transport agent (siderophore) pseudobactin enhance the growth of the potato and control certain phytopathogenic microorganisms. The structure of the title compound has been determined by single-crystal X-ray diffraction methods using counter data. The structure consisted of a linear hexapeptide, L-Lys-D-*threo*-β-OH-Asp-L-Ala-D-*allo*-Thr-L-Ala-D-N^{δ}-OH-Orn, in which the N^{δ}-OH nitrogen of the ornithine was cyclized with the C-terminal carboxyl group, and the N^{ϵ}-amino group of the lysine was linked via an amide bond to a fluorescent quinoline derivative. The iron-chelating groups consisted of a hydroxamate group derived from N^{δ}-hydroxyornithine, an α-hydroxy acid derived from β-hydroxyaspartic acid, and an *o*-dihydroxy aromatic group derived from the quinoline moiety. The combination of metal-chelating ligands and the alternating L- and D-amino acids was unusual. The title compound crystallized as a single coordination isomer with the Λ absolute configuration. The present study is the first structural determination of a fluorescent siderophore. In the crystal structure, ferric pseudobactin formed a dimer, which constituted the asymmetric unit. The asymmetric unit also contained 26 water molecules. The molecules in the dimer were related by a pseudo-2-fold symmetry axis. Red-brown crystals of ferric pseudobactin ($C_{42}H_{57}N_{12}O_{16}Fe\cdot 13H_2O$), obtained from pyridine–acetic acid buffer solution equilibrated with water, conformed to space group *I*2 with a = 29.006 (23) Å, b = 14.511 (13) Å, c = 28.791 (21) Å, and β = 96.06 (5)° at −135 (2) °C. For eight molecules per unit cell, the calculated density was 1.38 g/cm³; the observed density was 1.40 g/cm³. The structure was refined by least-squares methods with anisotropic thermal parameters for all nonhydrogen atoms to a final R factor of 0.08 (8989 observed reflections).

Specific strains of the *Pseudomonas fluorescens-putida* group have recently been used as seed inoculants on crop plants to promote growth and increase yields. These pseudomonads, termed plant growth promoting rhizobacteria (PGPR),[1] rapidly colonize plant roots of the potato, sugar beet, and radish and cause statistically significant yield increases (Kloepper et al.,

† From the Department of Chemistry, University of California at San Diego, La Jolla, California 92093 (M.T. and J.L.), and the Department of Chemistry, University of Oklahoma, Norman, Oklahoma 73019 (M.B.H., C.L.B., and D.v.d.H.). *Received March 24, 1981.* This work was supported in part by grants from the U.S. Public Health Service (AI 14084 and GM 21822) and National Institutes of Health (RR00719) to the Bioorganic, Biomedical Mass Spectrometry Resource (A. L. Burlingame, Director), Space Sciences Laboratory, University of California, Berkeley, CA 94720.

[1] Abbreviations used: PGPR, plant growth promoting rhizobacteria; PITC, phenyl isothiocyanate; CF_3COOH, trifluoroacetic acid; N^{δ}-OH-Orn, N^{δ}-hydroxyornithine; β-OH-Asp, β-hydroxyaspartic acid; KB, King's medium B; PTH, 3-phenyl-2-thiohydantoin; TLC, thin-layer chromatography; CD, circular dichroism; *I*, intensity; *F*, structure factor; rms, root mean square; W, water molecule.

0006-2960/81/0420-6446$01.25/0

1980c; Suslow et al., 1979). PGPR exert their plant growth promoting activity in part by depriving some native microflora of iron and thereby reducing microbial root colonization (Kloepper et al., 1980b). PGPR produce extracellular siderophores [microbial iron transport agents (Neilands, 1977)] which efficiently complex environmental iron, making it less available to certain native microflora, thus inhibiting their growth. In addition, PGPR are effective biological control agents of *Fusarium* wilt and take-all diseases, caused by the soil-borne fungi *Fusarium oxysporum* f. sp. *lini* and *Gaeumannomyces graminis* var. *tritici*, respectively (Kloepper et al., 1980a). Apparently, siderophores of PGPR deny iron(III) to these pathogens, thus inhibiting their growth.

We have isolated a yellow-green, fluorescent siderophore, designated pseudobactin, from plant growth promoting *Pseudomonas* B10. Pseudobactin has the same ability to enhance potato growth and control plant pathogens as *Pseudomonas* B10 (Kloepper et al., 1980a,b). We describe here the crystal and molecular structure of ferric pseudobactin.

Experimental Procedures

Materials. Phenyl isothiocyanate (PITC) (sequenation grade) was purchased from Eastman. Trifluoroacetic acid (CF_3COOH) and pyridine were distilled prior to use. Polyamide sheets (Cheng Chin) and dansyl chloride were obtained from Pierce. The DL-*threo*-β-hydroxyaspartic acid was obtained from Calbiochem-Behring, and N^{δ}-hydroxyornithine (N^{δ}-OH-Orn) was obtained by hydrolyzing 1-hydroxy-3-(*S*)-amino-2-piperidone (gift from Dr. J. B. Neilands) with 6 N HCl for 30 min at 110 °C (Akers & Neilands, 1973).

Isolation of Ferric Pseudobactin. Pseudomonas B10 was obtained from Dr. J. W. Kloepper, Department of Plant Pathology, University of California, Berkeley, and was maintained on King's medium B (KB) plates (King et al., 1954). An iron-deficient minimal medium consisting of 3 g of KH_2PO_4, 6 g of Na_2HPO_4, 5 g of NaCl, 1 g of NH_4Cl, and 10 mL of glycerol per L, and made 0.025% (w/v) in $MgSO_4 \cdot 7H_2O$ and 0.3% (w/v) in proteose peptone no. 3 (Difco), was used for the production of pseudobactin from *Pseudomonas* B10. A stock solution of proteose peptone no. 3 was deferrated with 8-hydroxyquinoline as described previously (Bell et al., 1979).

A single colony of *Pseudomonas* B10 was inoculated into 2 mL of KB medium, and the culture was shaken overnight at room temperature. Approximately 0.5 mL was transferred to 50 mL of minimal medium, and the culture was shaken overnight at room temperature. Approximately 5 mL each was transferred to eight 1-L portions of minimal medium, and the cultures were shaken for 2 days and were then harvested by centrifugation. After approximately 1 g of $Fe(NO_3)_3 \cdot 9H_2O$ was added per L of yellow-green, fluorescent culture supernatant fluids, the red-brown suspension was saturated with ammonium sulfate. The resulting slurry was extracted with benzyl alcohol and further treated by using a previously described procedure (Neilands, 1952). The red-brown aqueous extracts were concentrated to dryness in vacuo below room temperature. The residue was dissolved in 5 mL of pyridine and 25 mL of water, and the resulting solution was adjusted to pH 5.5 with glacial acetic acid. This solution was chromatographed at 4 °C on a column (2.5 × 100 cm) containing CM-Sephadex C-25, pyridinium form, equilibrated in 0.2 M pyridine–acetic acid buffer, pH 5.5. The predominant red-brown band consisted of ferric pseudobactin. After this solution was concentrated to dryness in vacuo, the residue was dissolved in 10 mL of pyridine and 30 mL of H_2O. The resulting solution was chromatographed at 4 °C on a column (5 × 100 cm) containing Bio-Gel P-2 (200–400 mesh, Bio-Rad Laboratories), equilibrated in 0.2 M pyridine–acetic acid buffer, pH 7.4. A small purple band consisting of ferric pseudobactin A (M. Teintze and J. Leong, unpublished experiments) eluted ahead of the predominant ferric pseudobactin-containing band. The red-brown band was concentrated to dryness in vacuo, and the residue was stored at 4 °C away from light. The yield was typically 150 mg/Liter of culture supernatant fluids.

The extinction coefficient of ferric pseudobactin at its absorption maximum was calculated from the absorbance of an aqueous solution whose iron concentration was determined by atomic absorption spectroscopy using a Varian AA-275 spectrophotometer in the flame mode.

Pseudobactin. Approximately 0.5 g of ferric pseudobactin was deferrated with 8-hydroxyquinoline as described previously (Meyer & Abdallah, 1978). After the yellow-green, fluorescent aqueous extract was concentrated to dryness in vacuo, the residue was dissolved in 5 mL of 0.2 M pyridine–acetic acid buffer, pH 5.5, and the resulting solution was chromatographed at 4 °C on a column (2.0 × 100 cm) containing Bio-Gel P-2 equilibrated in the same buffer. The yellow-green, fluorescent band was concentrated to dryness in vacuo. For spectroscopic measurements, pseudobactin was converted to the chloride salt at 4 °C by passing an aqueous solution through a short column containing DEAE-Sephadex A-25 (chloride form), equilibrated in water. The eluate was concentrated to dryness in vacuo, and the residue was stored under high vacuum at −70 °C away from light.

Chromic Pseudobactin. A 2–3-fold molar excess of solid chromous chloride (Pfaltz and Bauer) was added in one portion under nitrogen flush to a rapidly stirred deoxygenated solution of 5 mg of pseudobactin (chloride form) in 10 mL of methanol at room temperature. Immediately, 2.1 mg of sodium bicarbonate was added. The yellow-green suspension was stirred for 10 min, and then air was bubbled through it for 5 min. After the methanol had been removed in vacuo, 3 mL of water was added, and the solution was saturated with ammonium sulfate. The resulting suspension was extracted with benzyl alcohol and further treated as described above. After the yellow-green aqueous extract was concentrated to dryness in vacuo, the residue was dissolved in 1.0 mL of 0.2 M pyridine–acetic acid buffer, pH 7.4, and chromatographed at 4 °C on a column (1.5 × 80 cm) containing Bio-Gel P-2, equilibrated in the same buffer. A yellow chromium-containing band eluted ahead of the yellow band consisting of chromic pseudobactin. After the latter band was concentrated to dryness in vacuo, the residue was dissolved in water, and the resulting solution was stored at −20 °C away from light.

The extinction coefficient of chromic pseudobactin at its absorption maximum was calculated from the absorbance of an aqueous solution, whose chromium concentration was determined spectrophotometrically as $[CrO_4]^{2-}$ (ϵ_{372} = 4815 L mol^{-1} cm^{-1}) (Haupt, 1952) after oxidation of an aliquot with alkaline hydrogen peroxide. Excess hydrogen peroxide was removed by boiling the solution for 0.5 h.

Amino Acid Analyses. Analyses were carried out on a Beckman 117 amino acid analyzer with a single column. A final buffer, which consisted of 0.2 M sodium citrate and 0.8 M NaCl, pH 6.4, was used for optimum resolution of ornithine and lysine. Pseudobactin samples were hydrolyzed in vacuo for 18 h at 110 °C in distilled 6 N HCl or 47% HI.

Sequencing. Manual Edman degradations (Edman & Henschen, 1975) were carried out on 1–5 mg of pseudobactin in 3-mL glass-stoppered centrifuge tubes. Coupling with

phenyl isothiocyanate was performed in 50% pyridine at pH 9 for 1 h at 45 °C. This solution was extracted 5 times with 2 volumes of benzene and then freeze-dried. Cleavage was carried out in anhydrous CF_3COOH at 37 °C for 30 min under N_2. After the CF_3COOH was removed in vacuo, the thiazolinone amino acid released was separated from the remaining peptide. This required a different procedure for each step of the sequence, because of the unusual amino acids involved and the short length of the peptide. The first amino acid derivative was separated from the remaining peptide by chromatography at 4 °C on a Bio-Gel P-2 column (2.0 × 95 cm) equilibrated in 2.5 M pyridine–acetic acid buffer, pH 5.5. Each 5-mL fraction was assayed for iron-binding activity by adding 800 μL to 100 μL of 2.0% $Fe(ClO_4)_3 \cdot xH_2O$, followed by 100 μL of 1.0 M sodium phosphate buffer, pH 7.0. After the suspension was centrifuged at 10000*g* for 10 min, the absorbance of the supernatant fluids at 400 nm was measured. A yellow-green, fluorescent, iron-binding band eluted ahead of a colorless iron-binding band. The former band was further purified by high-voltage preparative paper electrophoresis (vide infra) in the same buffer. The amino acid derivative resulting from the second Edman cleavage was extracted with *n*-butyl acetate 5 times from an aqueous suspension, and the combined organic phases were back-extracted 3 times with H_2O. These water extracts, which contained some of the peptide, were pooled with the aqueous phase from the original extractions and were freeze-dried. In the third, fourth, and fifth steps of the sequence, the residue after cleavage was suspended in a small amount of water and then extracted 6–10 times with benzene. After each step, the phenylthiocarbamoyl- or 3-phenyl-2-thiohydantoin-amino acid (PTH) derivatives were back-hydrolyzed with 47% HI in vacuo at 130 °C for 18 h; an aliquot of the remaining peptide was also hydrolyzed under the same conditions. Both samples were run on the amino acid analyzer prior to proceeding.

At each step of the sequence, an aliquot of the peptide was removed, and the amino terminal was determined by the dansyl N-terminal method (Hartley, 1970) using 7.5 × 7.5 cm polyamide sheets. Dansyl-N^{δ}-hydroxyornithine and dansyl-*threo*-β-hydroxyaspartic acid standards were prepared by reaction of the corresponding amino acids with dansyl chloride.

Chromatography and Paper Electrophoresis. Thin-layer chromatography of the ferric and chromic complexes of pseudobactin was performed on silica gel 60F-254 TLC glass plates (EM Laboratories, Inc.) and Polygram Sil G plastic sheets (Brinkmann Instruments, Inc.) with 30% H_2O–CH_3OH (v/v) as the solvent system. TLC of pseudobactin was performed on Polygram Cell 300 and Polyamid-11 plastic sheets (Brinkmann Instruments, Inc.) with 1-butanol–acetic acid–water (3:1:1) (v/v/v) as the solvent system. Spots were detected visually or with ultraviolet illumination or were stained with iodine vapor. Pseudobactin could also be visualized by spraying plates with 0.1 M $FeCl_3 \cdot 6H_2O$ in 0.1 N HCl or with 0.1 M $K_3Fe(CN)_6$–0.1 M $FeCl_3 \cdot 6H_2O$ in 0.1 N HCl (1:1).

Descending paper chromatography was performed in 1-butanol–methyl ethyl ketone–water–NH_4OH (5:3:1:1) for 14 h (Dietzler & Strominger, 1973). Spots were visualized by dipping the dried chromatograms in 1% ninhydrin in acetone–1% cadmium acetate in 33% acetic acid (85:15).

Paper electrophoresis was carried out at either pH 6.5 (10% pyridine and 0.3% acetic acid), pH 3.5 (0.5% pyridine and 5% acetic acid), or pH 1.9 (8% acetic acid and 2% formic acid) in a high-voltage apparatus described previously (Ryler et al., 1955). Standards included ferrioxamine B (+1 ionic charge) (Leong & Raymond, 1975) and ferrichrome (neutral) (Neilands, 1952). Spots were visualized as described above. Pseudobactin and its metal complexes were homogeneous by TLC and electrophoresis of their solutions.

Table I: Crystal Data of Ferric Pseudobactin

$C_{42}H_{57}N_{12}O_{16}Fe \cdot 13H_2O$	
formula wt = 1276.04	
monoclinic, *I*2	
cell parameters (at −135 °C):	$a = 29.006$ (23) Å
	$b = 14.511$ (13) Å
	$c = 28.791$ (21) Å
	$\beta = 96.06$ (5)°
	$V = 12051$ Å^3
	$Z = 8$
$\rho_{calcd} = 1.38$ g/cm^3	
$\rho_{obsd} = 1.40$ g/cm^3	
$\mu = 3.6$ cm^{-1} (Mo $K\bar{\alpha}$ radiation)	

[a] Room temperature volume is assumed to be 1.02 × 12051 Å^3.

Spectroscopy. Visible spectra were measured with a Cary 17 spectrophotometer; infrared spectra were obtained as KBr pellets on a Nicolet 7000 FT-IR spectrophotometer; circular dichroism (CD) spectra were recorded on a Jasco J-10 spectropolarimeter; mass spectra were obtained in the electron-impact and field-desorption modes in the Space Sciences Laboratory, University of California, Berkeley.

Crystallization and Intensity Data Collection. Two different crystalline forms of ferric pseudobactin were observed. Monoclinic crystals with $a = 42.136$ Å, $b = 14.644$ Å, $c = 38.929$ Å, $\beta = 95.55°$, space group *A*2, and $Z = 16$ (four molecules per asymmetric unit) were obtained from solutions in dimethylformamide or dimethyl sulfoxide, equilibrated with water. However, another crystal form was obtained by diffusion of water into a solution of ferric pseudobactin in 2.5 M pyridine–acetic acid buffer, pH 5.5. These crystals were also monoclinic with space group *I*2 and $Z = 8$ (two molecules per asymmetric unit). This second form was used for the structure determination.

The crystals grown from pyridine–acetic acid buffer were found to undergo slow decomposition in open air. A well-formed prismatic crystal of dimensions 0.60 × 0.40 × 0.28 mm was mounted under the mother liquor and was placed in a cold N_2 beam (−135 °C) during the entire period of X-ray measurements. Preliminary investigation showed the crystal to be monoclinic with a centered cell. The C-centered cell showed a β angle of 138.2°, and therefore a body-centered cell ($\beta = 96.06°$) with space group *I*2 was taken as the working cell for the structure determination.

All crystallographic measurements on the crystal were performed with a Nonius CAD-4 counter diffractometer controlled by a PDP8/e computer and fitted with a low-temperature device. The crystal data of ferric pseudobactin are given in Table I.

The density of the crystal was determined at room temperature by the flotation method in a chloroform–diethyl ether solution. The cell parameters were obtained by a least-squares fit to the $+2\theta$ and -2θ values of 48 reflections measured at −135 °C with Mo $K\alpha_1$ radiation.

The intensities of all unique reflections with $2\theta \leq 53°$ were measured at −135 °C by using graphite-monochromatized Mo $K\bar{\alpha}$ radiation. A θ–2θ scan technique was employed with a scan angle of $(0.75 + 0.20 \tan \theta)°$ for each reflection. A horizontal aperture with a variable width of $(3.5 + 0.86 \tan \theta)$ mm and a constant height of 6 mm was placed at a distance of 173 mm from the crystal. Each reflection was scanned for a maximum time of 60 s, with two-thirds of the time spent scanning the peak and one-sixth of the time spent on each of the left and right backgrounds. The intensities of three re-

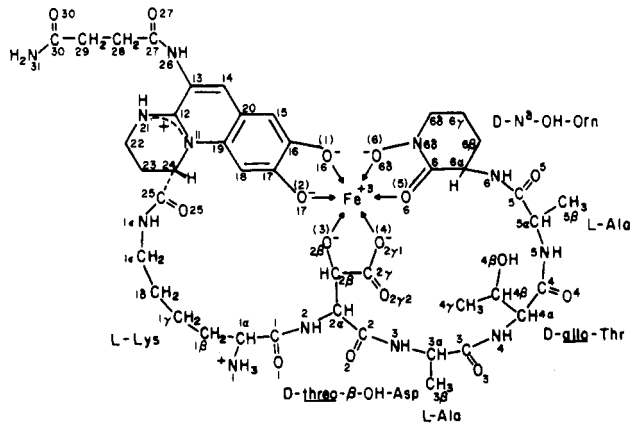

FIGURE 1: Schematic drawing of ferric pseudobactin showing the atom numbering scheme followed in the text.

flections were monitored every 5000 s. The maximum variation in monitor intensities was 4.5% during 14 days of data collection. The orientation of the crystal was checked after every 200 measurements, and a new orientation matrix was obtained if an angular change in the control reflections was more than 0.1°.

Of 12946 reflections measured, 8989 were considered "observed" [$I > 2\sigma(I)$]. The observed reflections were used in the structure determination and subsequent refinement. Intensities were corrected for Lorentz and polarization factors, but no absorption correction was made. Each structure amplitude was assigned an experimental weight, $w_F = 1/\sigma_F^2$, where σ_F was obtained from counting statistics (Ealick et al., 1975).

Structure Determination and Refinements. Repeated applications of direct methods as incorporated in the programs MULTAN (Germain et al., 1971) and SHELX (Sheldrick, 1976) failed to give any structural features which could be pursued. A three-dimensional Patterson map showed very distinct Fe–Fe vectors which gave an easy solution for the two iron positions. Structure factors were calculated with the iron positions by using partial data (6900 observed reflections with $2\theta \leq 46°$). This gave an R factor of 0.46. The iron positions were refined, and a difference map was calculated with heavy atom phases. Although the map showed a large number of peaks, only ten oxygen atoms bonded to iron atoms could be accepted with confidence. From this point onward, the complete structure was obtained by a process of successive difference Fourier syntheses. The amino acid sequence of pseudobactin, the presence of a fluorescent, phenolate-containing quinoline moiety attached to the ε-amino group of the lysine in the peptide, and the L-configuration of the alanines were known during the structure solution (vide infra; M. Teintze, unpublished experiments).

From the first few difference maps, parts of two peptide chains could be recognized. Complications resulted from the fact that the two independent molecules (termed molecule A and molecule B) formed a closely associated pair, related by a pseudo-2-fold axis. A turning point in the structure solution was the location of the two ortho oxygen atoms of the quinoline derivative that were bonded to the iron(III). The identification of atoms, particularly in the unknown quinoline moiety, was carried out by carefully scrutinizing peak heights in the difference maps and the isotropic thermal parameters of the atoms and their bond distances and angles. All atoms could then be identified with certainty except for atom 31 (Figure 1) of the quinoline moiety. It could be assigned either as an oxygen atom from a carboxylic acid or as a nitrogen atom from an amide group, but the overall charge of the ferric complex and the hydrogen bonding (vide infra) indicated the latter. The R factor at this stage was 0.22; all refinements up to this moment were carried out with the SHELX system. When the atoms were given anisotropic thermal parameters and the refinement was resumed with the full data (8989 observed reflections, $2\theta \leq 53°$), the problem became too large for the SHELX system. The rest of the refinement was carried out by using a block-diagonal least-squares program (Ahmed, 1966).

During the refinements, the primary amide group of the quinoline moiety in molecule A was found to be disordered. Repeated difference maps showed very low density peaks for the four terminal atoms [C(29), C(30), O(30), and N(31)] (Figure 1). These atoms were refined with fixed positions and assumed isotropic thermal parameters. Atom O(3), the carbonyl oxygen of L-alanine in molecule A, was also disordered. Difference maps showed two distinct peaks, and atom O(3) was therefore refined isotropically with fractional occupancy (55% and 45%) at two positions. A few water oxygen atoms with rather high temperature factors were refined isotropically as well. Both W(17) and W(24) lay close to a 2-fold symmetry axis. These two atoms were refined with 50% occupancy. All other atoms were refined anisotropically. Attempts to locate hydrogen atoms were only partially successful so hydrogen atom positions were calculated. Contributions from 60 such hydrogen atoms were included in the structure factor calculations. Anomalous dispersion effects due to iron atoms were incorporated into the F_o values. The L configuration of both alanine residues determined uniquely the absolute configuration of ferric pseudobactin. Two more cycles of refinement brought the final R factor down to 0.08. The total asymmetric unit consisting of 168 nonhydrogen atoms and a molecular weight of 2552 was thus resolved at atomic resolution. The refinement was discontinued when the maximum parameter shifts were less than 40% of the corresponding standard deviations. In all least-squares refinements, the quantity $\sum w_F(|kF_o| - |F_c|)^2$ was minimized. Scattering factors of Fe, C, O, and N atoms were taken from the *International Tables for X-ray Crystallography* (1974).

The final positional and equivalent isotropic thermal parameters of all nonhydrogen atoms are listed in Table II. The bond distances and bond angles calculated from the final positional parameters are listed in Tables III and A, respectively. Table A, a listing of structure factors, and anisotropic thermal parameters (Table B) are included in the supplementary material (see paragraph at end of paper).

Results

Physical Characteristics of Ferric Pseudobactin and Pseudobactin. Ferric pseudobactin was neutral upon electrophoresis at pH 6.5 and was only slightly soluble in water but was more soluble in pyridine–acetic acid buffers. Its absorption maximum at 400 nm was relatively insensitive to pH. The extinction coefficient, ϵ_{400}, was 2.1×10^4 L mol^{-1} cm^{-1}, assuming that ferric pseudobactin consists of one iron(III) per molecule (Figure 2). Its molecular weight based upon the extinction coefficient would be 1200 g/mol.

Pseudobactin had a migration somewhat less than that of ferrioxamine B upon electrophoresis at pH 6.5, indicating that it had a +1 ionic charge. Pseudobactin was very soluble in water; an aqueous solution of the chloride salt at pH 7.2 had an absorption maximum at 400 nm with a shoulder at 385 nm (Figure 2). The extinction coefficient, ϵ_{400}, was 1.5×10^4 L mol^{-1} cm^{-1}, using a molecular weight of 1024 g/mol as determined from the X-ray structure. The absorption maximum shifted to longer wavelengths, and the extinction coefficient became slightly greater as the pH increased from 3 to 9.

Table II: Positional and Equivalent Isotropic Thermal Parameters of Nonhydrogen Atoms[a]

atom	x (×10⁴)	y (×10⁴)	z (×10⁴)	U_{eq}[b]	atom	x (×10⁴)	y (×10⁴)	z (×10⁴)	U_{eq}[b]
				Nonhydrogen Atoms					
Fe	3222.7 (6)	−21.8 (13)	1532.9 (5)	0.0312 (8)	N(6)	3736 (3)	1055 (7)	166 (3)	0.038 (5)
	6264.3 (6)	334.4 (16)	3295.7 (6)	0.0420 (9)		6173 (4)	1294 (10)	4798 (4)	0.057 (7)
N(1)	1959 (3)	2116 (8)	2883 (3)	0.040 (6)	C(6α)	4040 (4)	383 (9)	402 (4)	0.036 (6)
	7187 (4)	2419 (8)	1686 (4)	0.048 (6)		5838 (5)	631 (14)	4657 (4)	0.071 (10)
C(1α)	2278 (4)	1595 (8)	2600 (4)	0.034 (6)	C(6)	3801 (4)	41 (9)	824 (3)	0.033 (6)
	6963 (4)	1805 (10)	2029 (4)	0.045 (7)		5914 (4)	312 (12)	4162 (4)	0.055 (8)
C(1)	1954 (4)	1123 (8)	2201 (4)	0.035 (6)	O(6)	3588 (2)	598 (5)	1059 (2)	0.031 (4)
	7354 (4)	1293 (11)	2339 (4)	0.052 (8)		6042 (3)	900 (7)	3869 (3)	0.050 (6)
O(1)	1560 (3)	938 (7)	2265 (3)	0.049 (5)	C(6β)	4164 (5)	−389 (10)	87 (4)	0.048 (7)
	7706 (3)	1076 (9)	2175 (3)	0.072 (7)		5825 (5)	−246 (16)	4979 (6)	0.087 (12)
C(1β)	2555 (4)	872 (8)	2889 (4)	0.036 (6)	C(6γ)	4386 (5)	−1180 (11)	398 (5)	0.059 (9)
	6633 (4)	1088 (10)	1775 (4)	0.046 (7)		5548 (6)	−1022 (17)	4721 (7)	0.108 (14)
C(1γ)	2927 (4)	1277 (9)	3255 (4)	0.042 (7)	C(6δ)	4045 (5)	−1569 (10)	697 (5)	0.054 (8)
	6242 (4)	1525 (10)	1472 (4)	0.045 (7)		5728 (7)	−1356 (15)	4311 (6)	0.093 (13)
C(1δ)	3191 (5)	495 (10)	3518 (5)	0.055 (8)	N(6δ)	3809 (4)	−837 (7)	921 (3)	0.039 (6)
	5904 (5)	796 (11)	1240 (5)	0.056 (8)		5887 (4)	−554 (9)	4030 (4)	0.061 (7)
C(1ε)	3550 (4)	807 (10)	3919 (4)	0.048 (8)	O(6δ)	3547 (3)	−1095 (6)	1267 (3)	0.041 (5)
	5507 (4)	1221 (11)	932 (4)	0.056 (8)		6012 (3)	−763 (8)	3606 (3)	0.064 (5)
N(1ε)	3935 (4)	1315 (8)	3742 (3)	0.046 (6)	N(11)	4465 (3)	2278 (8)	3145 (3)	0.037 (6)
	5222 (3)	1840 (8)	1185 (3)	0.046 (6)		4899 (3)	2932 (7)	1893 (3)	0.034 (5)
N(2)	2153 (3)	938 (7)	1825 (3)	0.033 (5)	C(12)	4592 (4)	3190 (10)	3219 (4)	0.046 (7)
	7249 (4)	1069 (8)	2755 (3)	0.043 (6)		4863 (4)	3831 (9)	1789 (4)	0.039 (7)
C(2α)	1911 (4)	388 (10)	1449 (4)	0.042 (7)	C(13)	4303 (4)	3868 (9)	3000 (4)	0.043 (7)
	7540 (4)	444 (10)	3080 (4)	0.046 (7)		5186 (4)	4459 (9)	2000 (4)	0.041 (7)
C(2)	1709 (4)	934 (11)	1028 (4)	0.049 (8)	C(14)	3941 (4)	3623 (10)	2681 (4)	0.041 (7)
	7853 (4)	975 (11)	3439 (4)	0.051 (8)		5555 (5)	4148 (10)	2280 (4)	0.051 (8)
O(2)	1457 (3)	558 (10)	727 (4)	0.085 (8)	C(15)	3483 (4)	2448 (8)	2221 (4)	0.029 (6)
	8120 (3)	565 (8)	3712 (3)	0.062 (6)		5999 (4)	2899 (10)	2685 (4)	0.046 (7)
C(2β)	2256 (4)	−353 (9)	1290 (4)	0.041 (7)	C(16)	3417 (4)	1543 (8)	2087 (3)	0.030 (6)
	7227 (4)	−156 (10)	3330 (4)	0.048 (8)		6035 (4)	1968 (9)	2809 (4)	0.038 (7)
O(2β)	2638 (2)	71 (6)	1122 (2)	0.036 (4)	O(16)	3099 (2)	1244 (5)	1760 (2)	0.029 (4)
	6919 (3)	338 (6)	3567 (2)	0.044 (5)		6393 (3)	1601 (6)	3066 (2)	0.039 (4)
C(2γ)	2398 (4)	−934 (9)	1721 (5)	0.044 (7)	C(17)	3742 (4)	846 (9)	2287 (3)	0.035 (6)
	6946 (4)	−791 (10)	2950 (4)	0.045 (7)		5657 (4)	1345 (9)	2654 (4)	0.040 (7)
O(2γ1)	2840 (3)	−890 (6)	1873 (3)	0.047 (5)	O(17)	3677 (2)	6 (6)	2115 (2)	0.035 (4)
	6529 (3)	−604 (7)	2852 (3)	0.057 (6)		5707 (3)	516 (6)	2820 (3)	0.048 (5)
O(2γ2)	2110 (3)	−1411 (7)	1903 (4)	0.062 (6)	C(18)	4090 (4)	1117 (9)	2645 (4)	0.037 (7)
	7150 (3)	−1448 (7)	2782 (3)	0.059 (6)		5284 (4)	1666 (8)	2354 (4)	0.033 (6)
N(3)	1822 (4)	1814 (9)	1017 (3)	0.051 (7)	C(19)	4132 (4)	2011 (9)	2784 (3)	0.031 (6)
	7831 (3)	1933 (8)	3439 (4)	0.047 (6)		5269 (4)	2585 (9)	2212 (4)	0.039 (7)
C(3α)	1646 (5)	2459 (14)	632 (5)	0.076 (10)	C(20)	3840 (4)	2713 (8)	2566 (4)	0.032 (6)
	8160 (4)	2457 (12)	3752 (4)	0.057 (9)		5615 (4)	3216 (9)	2377 (4)	0.042 (7)
C(3)	1823 (7)	2133 (16)	182 (5)	0.098 (13)	N(21)	4969 (4)	3423 (10)	3492 (4)	0.063 (8)
	8106 (4)	2267 (11)	4256 (4)	0.053 (8)		4512 (4)	4164 (8)	1501 (4)	0.055 (7)
O(3)[c]	1472 (7)	2142 (15)	−203 (7)	0.074 (6)	C(22)	5279 (5)	2712 (14)	3733 (5)	0.071 (10)
	1728 (8)	2711 (19)	−174 (9)	0.074 (7)		4149 (9)	3553 (16)	1313 (11)	0.188 (10)
	8441 (3)	2312 (9)	4555 (3)	0.072 (7)	C(23)	4971 (5)	1962 (12)	3884 (5)	0.057 (9)
C(3β)	1782 (7)	3457 (12)	770 (6)	0.084 (12)		4232 (5)	2643 (11)	1272 (6)	0.072 (2)
	8142 (6)	3459 (12)	3637 (6)	0.078 (11)	C(24)	4687 (4)	1551 (11)	3463 (4)	0.051 (8)
N(4)	2183 (4)	1673 (10)	178 (3)	0.060 (7)		4582 (4)	2213 (9)	1649 (4)	0.039 (6)
	7676 (3)	2080 (9)	4367 (3)	0.049 (6)	C(25)	4317 (5)	934 (10)	3643 (4)	0.048 (7)
C(4α)	2342 (4)	1246 (11)	−228 (4)	0.051 (8)		4859 (4)	1515 (10)	1391 (4)	0.044 (7)
	7582 (4)	1664 (13)	4811 (4)	0.060 (9)	O(25)	4427 (4)	112 (8)	3734 (4)	0.078 (7)
C(4)	2751 (4)	1726 (9)	−410 (4)	0.043 (7)		4721 (3)	733 (7)	1358 (4)	0.060 (6)
	7217 (4)	2198 (12)	5062 (4)	0.055 (8)	N(26)	4402 (4)	4809 (9)	3162 (4)	0.062 (8)
O(4)	2845 (3)	1631 (7)	−803 (3)	0.056 (6)		5119 (4)	5423 (8)	1902 (4)	0.051 (6)
	7238 (3)	2215 (10)	5483 (3)	0.077 (7)	C(27)	4436 (5)	5511 (13)	2886 (5)	0.063 (9)
C(4β)	2459 (5)	244 (12)	−97 (4)	0.058 (9)		5357 (5)	5852 (12)	1612 (6)	0.067 (10)
	7465 (4)	677 (11)	4732 (4)	0.052 (8)	O(27)	4391 (4)	5463 (9)	2461 (4)	0.077 (7)
O(4β)	2847 (3)	212 (6)	257 (3)	0.047 (5)		5639 (5)	5468 (10)	1348 (6)	0.121 (10)
	7011 (3)	597 (7)	4482 (3)	0.054 (5)	C(28)	4504 (7)	6382 (15)	3176 (7)	0.089 (6)
C(4γ)	2595 (7)	−354 (14)	−521 (5)	0.088 (12)		5281 (6)	6869 (10)	1561 (6)	0.067 (10)
	7457 (5)	141 (14)	5202 (5)	0.073 (10)	C(29)	4840 (0)[c]	7000 (0)	3020 (0)	0.189 (0)
N(5)	3028 (4)	2215 (8)	−78 (3)	0.047 (6)		5499 (6)	7257 (12)	1134 (5)	0.070 (10)
	6858 (4)	2555 (10)	4788 (4)	0.060 (7)	C(30)	5208 (0)[c]	7500 (0)	3229 (0)	0.189 (0)
C(5α)	3489 (5)	2529 (10)	−160 (4)	0.051 (8)		5293 (5)	6864 (11)	686 (5)	0.062 (10)
	6421 (5)	2874 (15)	4959 (5)	0.081 (11)	O(30)	5050 (0)[c]	7900 (0)	3490 (0)	0.189 (0)
O(5)	4272 (3)	2169 (7)	133 (3)	0.063 (7)		4891 (4)	6574 (9)	614 (4)	0.088 (8)
	5650 (4)	2354 (10)	4965 (4)	0.093 (9)	N(31)	5625 (0)[c]	7600 (0)	3073 (0)	0.189 (0)
C(5)	3857 (5)	1915 (9)	59 (4)	0.045 (6)		5587 (5)	6824 (10)	348 (4)	0.077 (9)
	6045 (5)	2127 (14)	4910 (4)	0.067 (10)					
C(5β)	3551 (6)	3572 (10)	11 (6)	0.071 (10)					
	6256 (6)	3794 (13)	4749 (7)	0.089 (12)					

Table II (*Continued*)

atom	x (×10⁴)	y (×10⁴)	z (×10⁴)	U_{eq} [b]	atom	x (×10⁴)	y (×10⁴)	z (×10⁴)	U_{eq} [b]
				Water Molecules					
W(1)	1711 (5)	622 (10)	3869 (6)	0.126 (11)	W(15)	5625 (4)	3665 (8)	1061 (4)	0.077 (7)
W(2)	55 (5)	4445 (12)	2073 (5)	0.124 (11)	W(16)	7250 (5)	3227 (11)	2854 (4)	0.113 (10)
W(3)	604 (4)	3712 (9)	2848 (5)	0.104 (10)	W(17)[c]	4906 (7)	3619 (14)	4813 (6)	0.060 (5)
W(4)	1548 (3)	3542 (7)	2264 (4)	0.067 (7)	W(18)	5410 (6)	5042 (15)	3777 (7)	0.167 (7)
W(5)	2483 (4)	3605 (7)	2116 (4)	0.067 (7)	W(19)	6803 (7)	4542 (17)	3412 (7)	0.185 (8)
W(6)	2044 (3)	2398 (7)	3859 (3)	0.052 (5)	W(20)	5034 (6)	−953 (13)	1544 (6)	0.135 (6)
W(7)	2917 (4)	3987 (7)	1337 (3)	0.071 (7)	W(21)	872 (6)	3399 (13)	1469 (6)	0.146 (6)
W(8)	974 (4)	1947 (10)	3078 (4)	0.088 (8)	W(22)	8183 (7)	3015 (17)	1113 (7)	0.190 (9)
W(9)	2929 (3)	2340 (7)	907 (3)	0.056 (6)	W(23)	8623 (7)	2399 (16)	2650 (7)	0.182 (8)
W(10)	765 (4)	935 (8)	3841 (4)	0.073 (7)	W(24)[c]	5101 (7)	3259 (14)	160 (6)	0.063 (6)
W(11)	4273 (5)	4530 (12)	4099 (5)	0.124 (11)	W(25)	5838 (8)	−1120 (18)	2078 (8)	0.203 (9)
W(12)	6806 (3)	2698 (7)	3794 (3)	0.063 (6)	W(26)	8302 (12)	1357 (29)	1477 (12)	0.328 (17)
W(13)	3648 (4)	3125 (8)	3771 (4)	0.073 (7)	W(27)	8707 (9)	1120 (20)	2607 (9)	0.237 (11)
W(14)	6599 (4)	3726 (8)	1303 (4)	0.077 (7)					

[a] Molecule A, upper values; molecule B, lower values. [b] $U_{eq} = (1/6\pi^2)\Sigma_i\Sigma_j\beta_{ij}\bar{a}_i\bar{a}_j$. [c] Disordered; see text.

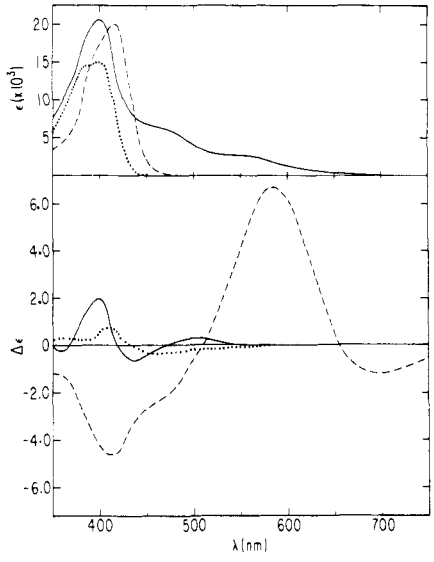

FIGURE 2: Absorption and CD spectra of pseudobactin (···), ferric pseudobactin (—), and chromic pseudobactin (- - -), all in aqueous solution.

Spectrophotometric titration of a solution of pseudobactin in 0.1 M sodium acetate buffer, pH 5.2, at 460 nm with 3.0 mM ferric ammonium sulfate gave an equivalent weight of 1100 g of ligand per mol of iron(III). This value suggests a ligand to iron(III) ratio of 1:1 for ferric pseudobactin.

Sequence of Pseudobactin. Amino acid analysis of a 6 N HCl hydrolysate of pseudobactin yielded 2 mol of alanine, 1 mol of lysine, 1 mol of threonine, and 1 mol of an unknown amino acid which eluted before aspartic acid on the amino acid analyzer. Analysis of a 47% HI hydrolysate yielded 2 mol of alanine, 1 mol of lysine, 1 mol of ornithine, 1 mol of threonine, and 1 mol of the unknown amino acid. The presence of ornithine in the reductive hydrolysate but not in the HCl hydrolysate indicated that pseudobactin contained 1 mol of N^{δ}-hydroxyornithine (Emery & Neilands, 1961). Paper electrophoresis of the hydrolysates at pH 6.5 and 1.9 gave one unidentified spot that stained orange with the ninhydrin–cadmium reagent. Authentic DL-*threo*-β-hydroxyaspartic acid showed an identical spot upon electrophoresis and had a retention time on the amino acid analyzer identical with that of the unknown amino acid in the pseudobactin hydrolysates. DL-*erythro*-β-Hydroxyaspartic acid is known to have significantly different behavior on the amino acid analyzer and when subjected to paper electrophoresis (Ikegami, 1975). The stereochemistry of the threonine, isolated by preparative paper electrophoresis at pH 1.9 of a 6 N HCl hydrolysate of pseudobactin, was determined by descending paper chromatography. Its R_f was identical with that of DL-*allo*-threonine, but different from that of DL-threonine. Both alanine residues were determined to have the L configuration by Dr. E. A. Hoopes at the Amino Acid Dating Laboratory, Scripps Institution of Oceanography, University of California, San Diego, as follows. A 6 N HCl hydrolysate of pseudobactin was reacted first with acidic methanol and then with *N*-(trifluoroacetyl)-L-prolyl chloride, and the alanine enantiomeric ratio was determined by gas–liquid chromatography of the resulting *N*-(trifluoroacetyl)-L-prolyl peptide methyl esters (Hoopes et al., 1978). Pseudobactin therefore contained 2 mol of L-alanine, 1 mol of *allo*-threonine, 1 mol of *threo*-β-hydroxyaspartic acid, 1 mol of lysine, and 1 mol of N^{δ}-hydroxyornithine.

Treatment of pseudobactin by the dansyl N-terminal method gave a monodansylated lysine. The Edman degradation of pseudobactin yielded a fluorescent amino acid derivative that migrated toward the cathode upon electrophoresis at pH 6.5, stained deep blue when sprayed with the ferricyanide reagent (a color indicative of phenolate compounds), and gave lysine upon back-hydrolysis with HI. The fluorescent group, therefore, had a positive charge and was attached via an amide bond to the ε-nitrogen of the N-terminal lysine. The remaining peptide was neutral upon electrophoresis at pH 6.5 and stained burgundy with the $FeCl_3$ reagent [a color characteristic of hydroxamate-containing compounds (Emery & Neilands, 1960)]. The second amino acid in the sequence was identified as *threo*-β-hydroxyaspartic acid by the methods described above. Mass spectral analysis of the second PTH-amino acid derivative yielded a parent and base peak at m/e 266, indicating that its side-chain carboxyl and hydroxyl groups were not substituted. The electrophoretic migration of the remaining peptide (residues 3–6) toward the cathode at pH 6.5 further substantiated the negative charge of the second residue. The sequence of the four remaining amino acids was determined to be -Ala-*allo*-Thr-Ala-N^{δ}-OH-Orn. The last amino acid still had a positive charge at pH 6.5 and still gave a burgundy color with the $FeCl_3$ spray, indicating that its carboxyl group was probably blocked and that it contained a hydroxamate group. Periodate oxidation (Emery & Neilands, 1960) of pseudobactin, however, did not yield any ether-extractable carboxylic acid, which would have been derived from the hydroxamate acyl group (data not shown). These findings were explained when the crystal structure of ferric pseudobactin (vide infra) showed that the carboxy-terminal N^{δ}-OH-

Table III: Bond Distances in Ferric Pseudobactin[a]

bond	molecule A	molecule B
	Peptide Chain	
N(1)-C(1α)	1.501 (15)	1.525 (17)
C(1α)-C(1)	1.563 (16)	1.556 (19)
C(1)-O(1)	1.207 (14)	1.211 (16)
C(1α)-C(1β)	1.516 (16)	1.544 (19)
C(1β)-C(1γ)	1.543 (17)	1.499 (18)
C(1γ)-C(1δ)	1.525 (19)	1.544 (20)
C(1δ)-C(1ε)	1.538 (19)	1.508 (19)
C(1ε)-N(1ε)	1.475 (17)	1.467 (18)
C(1)-N(2)	1.308 (14)	1.308 (16)
N(2)-C(2α)	1.463 (16)	1.497 (17)
C(2α)-C(2)	1.514 (18)	1.513 (19)
C(2)-O(2)	1.203 (17)	1.201 (16)
C(2α)-C(2β)	1.571 (18)	1.496 (19)
C(2γ)-O(2γ2)	1.245 (16)	1.247 (17)
C(2)-N(3)	1.319 (20)	1.392 (20)
N(3)-C(3α)	1.498 (20)	1.456 (18)
C(3α)-C(3)	1.521 (22)	1.500 (18)
C(3)-O(3)	1.330 (32)[b]	1.228 (16)
C(3α)-C(3β)	1.542 (27)	1.491 (25)
C(3)-N(4)	1.239 (24)[b]	1.347 (16)
N(4)-C(4α)	1.440 (17)	1.465 (17)
C(4α)-C(4)	1.517 (19)	1.549 (20)
C(4)-O(4)	1.200 (14)	1.206 (15)
C(4α)-C(4β)	1.530 (23)	1.484 (24)
C(4β)-O(4β)	1.439 (15)	1.438 (15)
C(4β)-C(4γ)	1.581 (22)	1.564 (21)
C(4)-N(5)	1.378 (16)	1.344 (17)
N(5)-C(5α)	1.455 (18)	1.481 (20)
C(5α)-C(5)	1.481 (19)	1.533 (25)
C(5)-O(5)	1.255 (17)	1.220 (18)
C(5α)-C(5β)	1.596 (21)	1.521 (28)
C(5)-N(6)	1.340 (17)	1.314 (23)
N(6)-C(6α)	1.436 (16)	1.395 (21)
C(6α)-C(6)	1.541 (15)	1.537 (19)
C(6α)-C(6β)	1.508 (18)	1.578 (27)
C(6β)-C(6γ)	1.553 (20)	1.529 (30)
C(6γ)-C(6δ)	1.490 (21)	1.426 (27)
C(6δ)-N(6δ)	1.452 (17)	1.515 (24)
	Quinoline Group	
N(11)-C(12)	1.384 (18)	1.341 (17)
C(12)-C(13)	1.399 (19)	1.401 (18)
C(13)-C(14)	1.367 (17)	1.348 (19)
C(14)-C(20)	1.385 (18)	1.389 (20)
C(20)-C(15)	1.411 (15)	1.423 (18)
C(15)-C(16)	1.377 (17)	1.399 (20)
C(17)-C(18)	1.419 (15)	1.393 (16)
C(18)-C(19)	1.359 (18)	1.395 (18)
C(19)-C(20)	1.426 (16)	1.404 (18)
N(11)-C(19)	1.397 (14)	1.428 (15)
N(11)-C(24)	1.496 (17)	1.512 (16)
C(12)-N(21)	1.321 (17)	1.333 (16)
N(21)-C(22)	1.492 (21)	1.437 (28)
C(22)-C(23)	1.501 (23)	1.349 (28)
C(23)-C(24)	1.515 (19)	1.540 (20)
C(24)-C(25)	1.529 (19)	1.532 (18)
C(25)-O(25)	1.255 (18)	1.204 (17)
C(25)-N(1ε)	1.296 (17)	1.346 (16)
C(13)-N(26)	1.462 (19)	1.435 (18)
N(26)-C(27)	1.303 (21)	1.297 (19)
C(27)-O(27)	1.219 (18)	1.299 (22)
C(27)-C(28)	1.516 (27)	1.497 (23)
C(28)-C(29)	1.431 (20)[b]	1.545 (23)
C(29)-C(30)	1.376[b]	1.477 (22)
C(30)-O(30)	1.088[b]	1.236 (19)
C(30)-N(31)	1.342[b]	1.359 (20)

[a] All distances are in angstroms. Standard deviations of least digits are within parentheses. Distances involved in iron coordination are shown in Figure 4. [b] Affected by disorder; see text.

Orn was cyclized like 1-hydroxy-3(*S*)-amino-2-piperidone (Akers & Neilands, 1973).

Infrared spectral analysis of pseudobactin showed an intense, broad absorption at 1650 cm^{-1} characteristic of amides, but none between 1700 and 1800 cm^{-1} where esters would absorb. This confirmed that none of the amino acid residues were esterified.

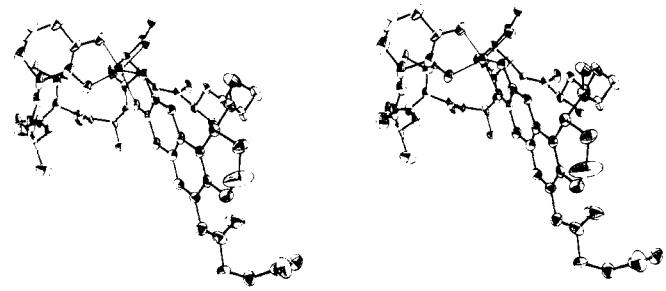

FIGURE 3: Stereoview of a single molecule of ferric pseudobactin (molecule B).

General Description of the Structure. The structure of ferric pseudobactin is shown schematically in Figure 1; a stereoview is shown in Figure 3. The molecular structure consisted of a linear hexapeptide, L-Lys-D-*threo*-β-OH-Asp-L-Ala-D-*allo*-Thr-L-Ala-D-N^{δ}-OH-Orn, in which the N^{ϵ}-amino group of lysine was attached by means of an amide group to the fluorescent quinoline derivative. The conformation of the molecule was stabilized by two strong intramolecular hydrogen bonds: one between the hydroxyl group of the threonine and the ionized hydroxyl group of the β-hydroxyaspartic acid [O(4β)-H···O(2β), 2.634 Å in molecule A and 2.647 Å in molecule B] and the other between the amide nitrogen of the β-hydroxyaspartic acid and one of the chelated oxygen atoms of the quinoline group [N(2)-H···O(16), 2.806 Å in molecule A and 2.834 Å in molecule B]. A weaker hydrogen bond occurred between the amide nitrogen of the N^{δ}-hydroxyornithine and the hydroxyl group of the threonine [N(6)-H···O(4β), 2.891 Å in molecule A and 2.868 Å in molecule B]. Molecules A and B were related by an approximate and noncrystallographic 2-fold symmetry axis at $x = {}^1/_2$, $z = {}^1/_4$ as seen from the positional parameters of the individual atoms in the two molecules (Table II).

Iron Coordination. The iron-binding ligands of ferric pseudobactin consisted of a hydroxamate moiety derived from N^{δ}-OH-Orn, an α-hydroxy acid group from β-OH-Asp, and an *o*-dihydroxy aromatic group from the fluorescent quinoline derivative. The bond distances and bond angles of the coordination octahedra in molecules A and B are shown in Figure 4. Both consisted of the same coordination isomer with the Λ absolute configuration. The ligand bite (the ratio of the O–O distances to the Fe–O distances) and the twist angle (60° for an ideal octahedron and 0° for the trigonal prismatic arrangement), which are used to describe the metal coordination, are listed in Table IV for each chelating group of ferric pseudobactin. The interplanar angle between the planes of atoms defining the two unique trigonal faces perpendicular to the pseudo-3-fold axis was 4° in molecule A and 6° in molecule B.

Peptide Chain. The peptide of pseudobactin was bent around the iron(III), forming a semicircular backbone (Figure 3). The ψ angles (IUPAC–IUB Commission, 1970) along the peptide backbone ranged between ±35°, except that of L-lysine (Table V); these angles resulted in an unusual conformation wherein successive amide nitrogens were cis (eclipsed). All peptide bonds were trans, with a maximum deviation of ω about 15° from the ideal value of 180°. The conformational angles, ω_j, ϕ_j, and ψ_j, in the peptide chain are listed in Table V.

There were differences in the individual bond lengths and angles among the different amino acid residues. The average

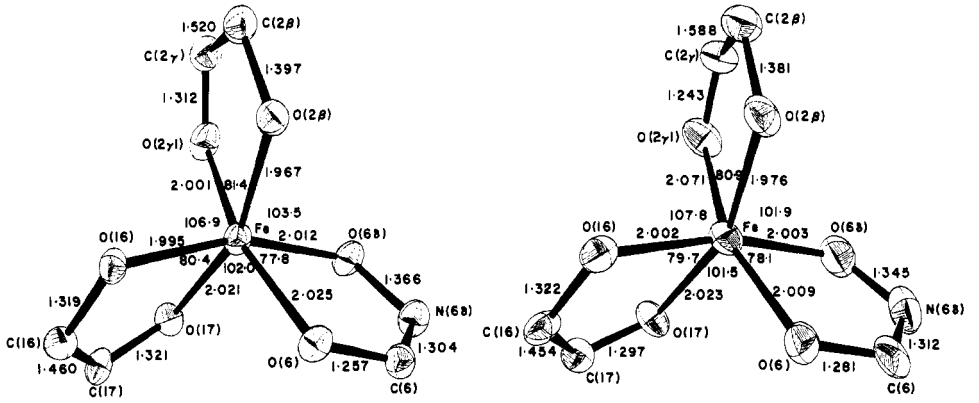

FIGURE 4: Geometry and dimensions of the iron coordination octahedron in molecule A (left) and in molecule B (right). Standard deviations ranged from 0.008 to 0.011 Å for Fe–O distances and from 0.014 to 0.021 Å for other distances.

Table IV: Comparison of Structural Parameters of Chelate Rings in Some Known Siderophores

				ferric pseudobactin		
parameter	ferrichrome[a]	ferrichrome A[a]	ferrioxamine E[a]	hydroxamate	α-hydroxy acid	*o*-dihydroxy aromatic
Fe–O(N) (Å)	1.983 (10)	1.980 (6)	1.953 (9)	2.008 (10)		
Fe–O(C) (Å)	2.034 (6)	2.033 (6)	2.055 (2)	2.017 (8)		
N–O(N) (Å)	1.389 (9)	1.373 (5)	1.381 (3)	1.356 (14)		
C–O(C) (Å)	1.278 (6)	1.265 (5)	1.275 (3)	1.269 (16)		
O···O (Å)	2.534 (10)	2.527 (7)	2.549 (3)	2.535 (16)	2.610 (15)	2.585 (14)
ligand bite	1.26	1.26	1.27	1.26	1.30	1.28
twist (deg)	42.9	41.4	45.1	41.4	36.4	37.8
O–Fe–O (deg)	78.2 (5)	78.0 (1)	78.9 (1)	78.0 (4)	81.2 (3)	80.1 (4)

[a] These siderophores contain only hydroxamate chelate rings. Standard deviations are in parentheses.

Table V: Torsion Angles in the Peptide Chain[a]

amino acid residue	φ	ψ	ω
L-Lys		−84	172
		−86	170
D-*threo*-β-OH-Asp	103	8	−179
	98	2	−174
L-Ala	−64	−26	172
	−63	−33	164
D-*allo*-Thr	106	26	165
	129	38	164
L-Ala	−99	20	−176
	−95	10	−167
D-N^{δ}-OH-Orn	126	13	
	121	11	

[a] All values are in degrees. Molecule A, upper values; molecule B, lower values.

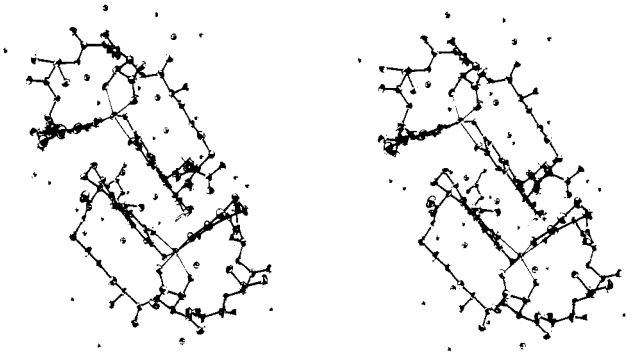

FIGURE 5: Stereoview of a dimeric pair including the surrounding water molecules. Molecule A is at the bottom, molecule B is at the top.

dimensions (without the disordered alanyl residue in molecule A) of all the amino acid residues were C–N = 1.339, C^{α}–N = 1.468, C^{α}–C = 1.527, and C–O = 1.225 Å. These values were in excellent agreement with those observed in other small linear and cyclic peptides (Marsh & Donohue, 1967; Hossain & van der Helm, 1978).

Quinoline Moiety. The two aromatic rings in the quinoline group were planar; the root mean square (rms) deviation of individual atoms from the least-squares plane through the ten atoms was 0.07 Å in molecule A and 0.06 Å in molecule B. A least-squares plane through the 14 atoms of the three-ring system had an rms deviation of 0.23 Å in molecule A and 0.12 Å in molecule B. The bond lengths and bond angles in the aromatic system were comparable to those observed in other related derivatives (Lerbcher & Trotter, 1972). The C(12)–N(21) bond distance was 1.321 Å in molecule A and 1.333 Å in molecule B, whereas the C(12)–N(11) bond distance was 1.384 Å in molecule A and 1.341 Å in molecule B. The similarity in the two C–N bond distances suggests that the positive charge was delocalized over all three atoms. Atom N(21) in ferric pseudobactin was ascertained to be trigonally substituted from its bond angles and a hydrogen atom attached to it in both molecules. These hydrogens were located in a difference Fourier map.

The succinyl diamide moiety of the quinoline group in molecule A was partially disordered. In molecule B, the bond lengths and bond angles in the primary amide moiety [C(29)–C(30), 1.477 Å; C(30)–O(30), 1.236 Å; C(30)–N(31), 1.359 Å; N(31)–C(30)–O(30), 121.2°] were in excellent agreement with those observed in the structure of acetamide (Denne & Small, 1971) and hence confirmed the assignment of atom 31 as a nitrogen atom.

Dimer. The two molecules in the asymmetric unit were packed close together, forming a dimeric unit. A stereoview of the pair is shown in Figure 5. The exterior boundaries of the dimer consisted of the hydrophilic peptide chains at opposite ends, the lipophilic lysine side chains on opposite sides,

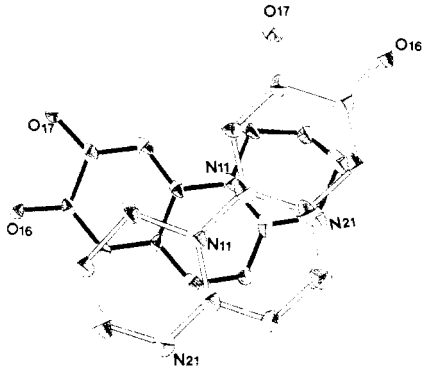

FIGURE 6: Overlap of quinoline aromatic systems within a dimeric pair. Molecule A (solid bonds); molecule B (hollow bonds).

and the succinic diamides at the bottom, whereas the iron atoms were located at the top and were accessible. The molecules were related by a pseudo-2-fold axis, which was approximately parallel to the pseudo-3-fold axes of the ferric coordination spheres. The Fe–Fe distance between the two molecules was 9.7 Å with no intervening groups along the Fe–Fe vector. Some apparent differences in bond lengths and angles between the two molecules were primarily due to disordered atoms. The dimer was stabilized by a hydrogen bond of 2.786 Å between N(26)–H of molecule B and O(27) of molecule A. The stacking overlap of the quinoline aromatic moieties of molecule A and molecule B is shown in Figure 6. The least-squares planes calculated through the atoms of the aromatic rings and O(16), O(17), N(21), and C(24) were at an angle of 15° and were separated by an average distance of about 3.6 Å. Atoms O(16) and O(17) were precluded from intimate involvement in the stacking since they were involved in iron chelation, but N(11) and N(21) of molecule A closely overlaid the adjacent aromatic ring system. Although the interplanar separation distance in the present structure was relatively large (Bugg et al., 1971) for a strong charge transfer interaction, the overlap of the aromatic systems may play a part in the packing of the dimer.

A stereoview of the least-squares fit of the two molecules is shown in Figure 7. The conformational similarity between the molecules was obvious. The only significant difference lay in the orientations of the succinyl diamide moieties with respect to the aromatic part of the quinoline groups.

Hydrogen Bonding and Crystal Packing. In addition to the three intramolecular hydrogen bonds within each of the molecules A and B, and the intermolecular hydrogen bond between the two molecules in the dimer described above, there were also four hydrogen bonds between adjacent B molecules [N(1)-H···$O(2\gamma_2)_{ii}$, 2.851 Å; N(31)-H···$O(3)_{ii}$, 2.893 Å; N-(31)-H′···$O(30)_i$, 2.987 Å; and $O(30)$···H-$N(31)_i$, 2.987 Å] and one hydrogen bond between N(1)-H′ of molecule B and $O(4)_i$ of a symmetry-related molecule A (2.781 Å) where $i = 1 - x, y, -z$ and $ii = 1^1/_2 - x, {}^1/_2 + y, {}^1/_2 - z$, and H and H′ are two different hydrogen atoms located on the atom of interest. The two hydrogen bonds to atom 31 further corroborated its assignment as a nitrogen atom. A total of 17 hydrogen bonds occurred between water molecules and molecule A and 19 between water molecules and molecule B. A total of 23 hydrogen bonds were found between water molecules. All amide NH and CO groups in the two molecules were involved in hydrogen bonding with the exception of O(1) and N(3) of molecule A.

Thus, the 26 water molecules in the asymmetric unit participated in extensive hydrogen bonding with molecules A and B and may have influenced the crystal packing.

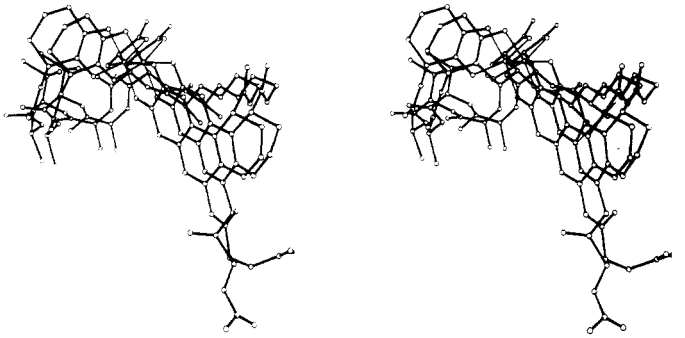

FIGURE 7: Stereoview of superimposed molecule A (right) and molecule B (left) separated from each other by a translation of 1 Å.

Chromic Pseudobactin. An examination of CPK molecular models of ferric pseudobactin indicated that only the eight coordination isomers with the Λ absolute configuration (Figure 8) and the Δ coordination isomers of V, VI, VII, and VIII were feasible. Since high-spin d^5 octahedral ferric siderophore complexes have no crystal-field stabilization energy, they are kinetically labile (Leong & Raymond, 1975). Ferric pseudobactin in solution could thus consist of several coordination isomers in rapid equilibrium. Replacement of ferric ion by chromic ion, which has a large crystal-field stabilization energy, should induce kinetic inertness and thereby allow the separation of coordination isomers that exist in an equilibrium mixture.

Gel filtration chromatography of crude chromic pseudobactin yielded two yellow chromium-containing bands. The faster eluting band remained at the origin on TLC, whereas the slower eluting band had an R_f identical with that of ferric pseudobactin. All coordination isomers of chromic pseudobactin would be neutral and expected to migrate on TLC. Since they would also be the same size and should have the same elution time on gel filtration, only the slower eluting band consisted of the desired chromic complex. The absorption maximum of the chromic complex was at 416 nm ($\epsilon = 2.0 \times 10^4$ L mol^{-1} cm^{-1}) (Figure 2). Chromic pseudobactin had bands in the CD spectrum at 412 (−4.6), 582 (6.8), and 702 (−1.2) nm ($\Delta\epsilon$), whereas ferric pseudobactin had bands at 400 (2.0), 436 (−0.8), and 502 (0.3) nm. The CD spectrum of pseudobactin at pH 7.2 had bands at 410 (0.8) and 460 (−0.3) nm and was very pH dependent.

Discussion

Yellow-green, fluorescent siderophores have been isolated from various *Pseudomonas* species, but none have been characterized structurally (Meyer & Abdallah, 1978; Cox & Graham, 1979; Liu & Shokrani, 1978; McCracken & Swinburne, 1979). None of the three different chelating groups found in ferric pseudobactin have been observed previously in siderophores, and this established the compound as unique. The chelating groups were similar, however, to those found in some other siderophores. The β-hydroxyaspartic acid was similar to the α-hydroxy acid present in schizokinen (Mullis et al., 1971) and aerobactin (Gibson & Magrath, 1969); the *o*-dihydroxyquinoline moiety was similar to the *o*-dihydroxybenzoyl groups found in enterobactin (Pollack & Neilands, 1970), agrobactin (Ong et al., 1979; Eng-Wilmot & van der Helm, 1980), and a number of other siderophores. Another cyclized N^{δ}-hydroxyornithine, 1-hydroxy-3(*S*)-amino-2-piperidone, has been isolated from the yeast *Rhodotorula pilimanae* (Akers & Neilands, 1973) but has not been shown

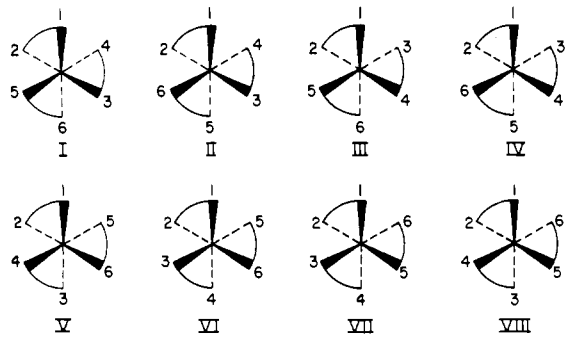

FIGURE 8: Eight Λ coordination isomers of ferric pseudobactin. The corresponding eight Δ isomers are not shown. The oxygen donor atoms are numbered as described in Figure 1. Ferric pseudobactin crystallized as isomer I with the Λ absolute configuration.

to be a siderophore. The alternating L- and D-amino acids in the pseudobactin sequence were also unusual and could explain why pseudobactin was not affected by trypsin, chymotrypsin, pepsin, Pronase, or leucine aminopeptidase under conditions where control peptides were completely digested (data not shown). This feature would effectively protect pseudobactin against degradation by other organisms. D-Amino acids have been observed in a new siderophore from the fungus *Neurospora crassa* (Eng-Wilmot et al., 1980) and in the *Pseudomonas* siderophore ferribactin, whose structure is unknown (Maurer et al., 1968).

The fluorescent quinolinyl chromophore in pseudobactin (Figure 1) is similar in structure to the one shown below (Corbin et al., 1970).

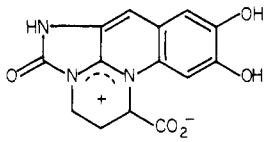

This chromophore was obtained upon acid hydrolysis of a yellow-green, fluorescent peptide isolated from culture supernatant fluids of *Azotobacter vinelandii* grown under iron-deficient conditions (Bulen & LeComte, 1962). The iron-binding properties of the *Azotobacter* peptide have not been reported, but it could be using the *o*-dihydroxy aromatic moiety of the fluorescent chromophore and a β-hydroxyaspartic acid residue also known to be present (Bulen & LeComte, 1962) as iron-binding ligands. This compound may therefore be a siderophore, like pseudobactin, but its amino acid composition is different. The compound N^2,N^6-bis(2,3-dihydroxybenzoyl)-L-lysine is believed to be a siderophore in *A. vinelandii* (Corbin & Bulen, 1969).

The metal coordination parameters, i.e., the ligand bite and twist angle, of the three different chelating groups of ferric pseudobactin are compared with those of other ferric siderophores in Table IV. The values for the hydroxamate group were similar to those found in ferrichrome (van der Helm et al., 1980), *N*,*N*′,*N*″-triacetylfusarinine (Hossain et al., 1980), and ferrioxamine E (van der Helm & Poling, 1976). The twist angles for the *o*-dihydroxy aromatic group and the β-hydroxyaspartic acid moiety were nearly identical and compare favorably to the 44.7° angle observed for the catecholate dianion in tris(catecholato)ferrate(III) (Raymond et al., 1976). The twist angles of the three chelating groups of ferric pseudobactin suggest that the geometry of the ferric complex is a distorted octahedron intermediate between a trigonal prism and an octahedron.

Chromic pseudobactin should consist of the same coordination isomer(s) as its ferric complex (vide infra). Since the high-spin d^4 octahedral reaction intermediate chromous pseudobactin had little crystal-field stabilization energy and therefore would be kinetically labile, all of its possible coordination isomer(s) would be in rapid equilibrium in solution. Exposure of this solution to air would have trapped each isomer in the chromic state.

The spin-allowed d–d $^4A_{2g} \rightarrow {}^4T_{1g}$ and $^4A_{2g} \rightarrow {}^4T_{2g}$ transitions of chromic pseudobactin were not observed. If the chromic complex is assumed to have d–d absorption maxima similar to those of other chromic siderophore complexes containing six octahedrally coordinated oxygens (Leong & Raymond, 1974a; Harris et al., 1979), its $^4A_{2g} \rightarrow {}^4T_{1g}$ transition was probably obscured by the intense ligand-based absorption band at 416 nm. The $^4A_{2g} \rightarrow {}^4T_{2g}$ transition, which would be expected to occur at approximately 580 nm, was apparently too weak to be observed. Nevertheless, the CD transitions of chromic pseudobactin at 582 and 702 nm were attributed to the $^4A_{2g} \rightarrow {}^4T_{2g}$ manifold, whereas the CD band at 412 nm could be derived from the $^4A_{2g} \rightarrow {}^4T_{1g}$ transition (Leong & Raymond, 1974a). Since the chromic complex has similar CD maxima and intensities as those of Λ-chromic deferriferrichrome, which has CD maxima at 432 (−2.49), 571 (7.47), and 661 (−1.74) nm (Δε) (Leong & Raymond, 1974b), the coordination isomer(s) of chromic pseudobactin must have the Λ absolute configuration. By analogy, the coordination isomer(s) of ferric pseudobactin should also have the Λ configuration in solution.

Since ferric and chromic pseudobactin both gave only one spot with identical R_f values upon TLC, both complexes probably consisted of the same Λ optical isomer in solution. This isomer would be the same one found in the X-ray structure. If more than one coordination isomer had been present, the isomers of the chromic complex should have been separable on TLC, since all of the isomers are diastereoisomers. However, the possibility that the chromic complex consisted of more than one diastereoisomer with the same R_f value on TLC cannot be ruled out.

The visible and CD spectra of ferric pseudobactin (Figure 2) are interpreted as follows. In addition to the strong absorption band at 400 nm, which appeared to be due to the fluorescent chromophore, shoulders were also observed at 460 (6×10^3) and 540 (3×10^3) nm (ε) and were most likely ligand to metal charge transfer bands. The CD bands at 436 and 502 nm appeared to be derived from the charge transfer absorption at 460 nm and are qualitatively similar to those of Λ-ferrichrome (van der Helm et al., 1980). However, the CD intensities of ferric pseudobactin were about an order of magnitude less than those of ferrichrome. It has been observed that the Λ coordination isomer of *N*,*N*′,*N*″-triacetylfusarinine observed in the crystalline state isomerizes upon dissolution to the predominant Δ isomer (Hossain et al., 1980). Therefore, the possibility that ferric pseudobactin consisted of a mixture of Δ and Λ coordination isomers in solution, with the Λ isomers predominating, although believed unlikely for the reasons cited above, cannot be eliminated.

The CD spectrum of pseudobactin (Figure 2) cannot be directly compared to or subtracted from those of the metal complexes because it was very pH dependent. At the high pH required to achieve the same ionization state found in its metal complexes, pseudobactin was not stable. Therefore, pseudobactin's contribution to the CD spectrum of ferric pseudobactin cannot be ascertained. The pH dependence of the visible and

CD spectra of pseudobactin was probably due to ionization of one of the phenolate protons.

At least two strategies can be envisioned to promote plant growth and/or control phytopathogenic microorganisms. These include the inoculation of soils with PGPR such as *Pseudomonas* B10 or the application of plant growth promoting siderophores such as pseudobactin to soils. A detailed knowledge of the antagonism of PGPR and their siderophores against plant pathogens will be needed before any strategy can be adopted on a widespread basis. Pseudobactin is known to exhibit in vitro antibiosis against certain rhizoplane phytopathogens, but not against others (Kloepper et al., 1980a,b; J. Leong, unpublished experiments). In order to determine what factors make pathogens susceptible to pseudobactin and other plant growth promoting siderophores, we have begun a program to ascertain the chemical structures of phytopathogenic siderophores, their equilibrium iron-binding constants, the efficiency of their iron assimilation systems, and their ability to utilize iron(III) from saprophytic siderophores. These properties of plant pathogens will be contrasted with those of PGPR. As a beginning, the mechanism by which iron uptake is facilitated by pseudobactin in *Pseudomonas* B10 was investigated (J. Leong, unpublished experiments).

Added in Proof

The structure of pyochelin, the siderophore of *Pseudomonas aeruginosa* PAO-1, has recently been reported (Cox et al., 1981), but it bears little resemblance to that of pseudobactin.

Acknowledgments

We thank Drs. H. A. Itano and R. F. Doolittle for the use of their equipment and Dr. E. A. Hoopes and K. M. Straub for experimental assistance.

Supplementary Material Available

Tables of the anisotropic thermal parameters for all nonhydrogen atoms and of the bond angles and a listing of all observed and calculated structure factors (46 pages). Ordering information is given on any current masthead page.

References

Ahmed, F. R. (1966) SFLS Program, NRC-10, National Research Council, Ottawa, Canada.

Akers, H. A., & Neilands, J. B. (1973) *Biochemistry 12*, 1006–1010.

Bell, S. J., Friedman, S. A., & Leong, J. (1979) *Antimicrob. Agents Chemother. 15*, 384–391.

Bugg, C. E., Thomas, J. M., Sundaralingam, M., & Rao, S. T. (1971) *Biopolymers 10*, 175–219.

Bulen, W. A., & LeComte, J. R. (1962) *Biochem. Biophys. Res. Commun. 9*, 523–528.

Corbin, J. L., & Bulen, W. A. (1969) *Biochemistry 8*, 757–762.

Corbin, J. L., Karle, I. L., & Karle, J. (1970) *J. Chem. Soc. D*, 186–187.

Cox, C. D., & Graham, R. (1979) *J. Bacteriol. 137*, 357–364.

Cox, C. D., Rinehart, K. L., Jr., Moore, M. L., & Cook, J. C., Jr. (1981) *Proc. Natl. Acad. Sci. U.S.A. 78*, 4256–4260.

Denne, W. A., & Small, R. W. H. (1971) *Acta Crystallogr. Sect. B B27*, 1094–1098.

Dietzler, D. N., & Strominger, J. L. (1973) *J. Biol. Chem. 248*, 104–109.

Ealick, S. E., van der Helm, D., & Weinheimer, A. J. (1975) *Acta Crystallogr., Sect. B B31*, 1618–1626.

Edman, P., & Henschen, A. (1975) *Mol. Biol., Biochem. Biophys. 8*, 232–279.

Emery, T., & Neilands, J. B. (1960) *J. Am. Chem. Soc. 82*, 3658–3662.

Emery, T., & Neilands, J. B. (1961) *J. Am. Chem. Soc. 83*, 1626–1628.

Eng-Wilmot, D. L., & van der Helm, D. (1980) *J. Am. Chem. Soc. 102*, 7719–7725.

Eng-Wilmot, D. L., Rahman, A., Mendenhall, J. V., Grayson, S. L., & van der Helm, D. (1980) Abstracts, 28th Southwest-32nd Southeast Regional Meeting of the American Chemical Society, No. 536, New Orleans, LA.

Germain, G., Main, P., & Woolfson, M. M. (1971) *Acta Crystallogr. Sect. A A27*, 368–376.

Gibson, F., & Magrath, D. I. (1969) *Biochim. Biophys. Acta 192*, 175–184.

Harris, W. R., Carrano, C. J., & Raymond, K. N. (1979) *J. Am. Chem. Soc. 101*, 2722–2727.

Hartley, B. S. (1970) *Biochem. J. 119*, 805–822.

Haupt, G. W. (1952) *J. Res. Natl. Bur. Stand. 48*, 414.

Hoopes, E. A., Peltzer, E. T., & Bada, J. L. (1978) *J. Chromatogr. Sci. 16*, 556–560.

Hossain, M. B., & van der Helm, D. (1978) *J. Am. Chem. Soc. 100*, 5191–5198.

Hossain, M. B., Eng-Wilmot, D. L., Loghry, R. A., & van der Helm, D. (1980) *J. Am. Chem. Soc. 102*, 5766–5773.

Ikegami, T. (1975) *Acta Med. Okayama 29*, 241–247.

International Tables for X-ray Crystallography (1974) Vol. IV, p 73, Kynoch Press, Birmingham, England.

IUPAC–IUB Commission on Biochemical Nomenclature (1970) *Biochemistry 9*, 3471–3483.

King, E. O., Ward, M. K., & Raney, D. E. (1954) *J. Lab. Clin. Med. 44*, 301–307.

Kloepper, J. W., Leong, J., Teintze, M., & Schroth, M. N. (1980a) *Curr. Microbiol. 4*, 317–320.

Kloepper, J. W., Leong, J., Teintze, M., & Schroth, M. N. (1980b) *Nature (London) 286*, 885–886.

Kloepper, J. W., Schroth, M. N., & Miller, T. D. (1980c) *Phytopathology 70*, 1078–1082.

Leong, J., & Raymond, K. N. (1974a) *J. Am. Chem. Soc. 96*, 1757–1762.

Leong, J., & Raymond, K. N. (1974b) *J. Am. Chem. Soc. 96*, 6628–6630.

Leong, J., & Raymond, K. N. (1975) *J. Am. Chem. Soc. 97*, 293–296.

Lerbcher, J. A., & Trotter, J. (1972) *J. Cryst. Mol. Struct. 2*, 67–77.

Liu, P. V., & Shokrani, F. (1978) *Infect. Immun. 22*, 878–890.

Marsh, R. E., & Donohue, J. (1967) *Adv. Protein Chem. 22*, 235–256.

Maurer, B., Müller, A., Keller-Schierlein, W., & Zähner, H. (1968) *Arch. Mikrobiol. 60*, 326–339.

McCracken, A. R., & Swinburne, T. R. (1979) *Physiol. Plant Pathol. 15*, 331–340.

Meyer, J. M., & Abdallah, M. A. (1978) *J. Gen. Microbiol. 107*, 319–328.

Mullis, K. B., Pollack, J. R., & Neilands, J. B. (1971) *Biochemistry 10*, 4894–4898.

Neilands, J. B. (1952) *J. Am. Chem. Soc. 74*, 4846–4847.

Neilands, J. B. (1977) *Adv. Chem. Ser. No. 162*, 3–32.
Ong, S. A., Peterson, T., & Neilands, J. B. (1979) *J. Biol. Chem. 254*, 1860–1865.
Pollack, J. R., & Neilands, J. B. (1970) *Biochem. Biophys. Res. Commun. 38*, 989–992.
Raymond, K. N., Isied, S. S., Brown, L. D., Fronczek, F. R., & Nibert, J. H. (1976) *J. Am. Chem. Soc. 98*, 1767–1774.
Ryler, A. P., Sanger, F., Smith, L. F., & Kitai, R. (1955) *Biochem. J. 60*, 541–556.
Sheldrick, G. (1976) *SHELX-76*, University Chemical Laboratory, Cambridge.
Suslow, T. V., Kloepper, J. W., Schroth, M. N., & Burr, T. J. (1979) *Calif. Agric. 33*, 15–17.
van der Helm, D., & Poling, M. (1976) *J. Am. Chem. Soc. 98*, 82–86.
van der Helm, D., Baker, J. R., Eng-Wilmot, D. L., Hossain, M. B., & Loghry, R. A. (1980) *J. Am. Chem. Soc. 102*, 4224–4231.

Structure of Pseudobactin A, a Second Siderophore from Plant Growth Promoting *Pseudomonas* B10†

Martin Teintze and John Leong*

ABSTRACT: The structure of nonfluorescent pseudobactin A, one of two extracellular siderophores (microbial iron transport agents) produced by the plant growth promoting bacterium *Pseudomonas* B10, was determined by comparison of its ^1H and ^{13}C NMR spectra with those of yellow-green, fluorescent pseudobactin, the other siderophore. The molecular and crystal structure of ferric pseudobactin is reported in the preceding paper in this issue [Teintze, M., Hossain, M. B., Barnes, C. L., Leong, J., & van der Helm, D. (1981) *Biochemistry* (preceding paper in this issue)]. The only structural difference between pseudobactin and pseudobactin A was that the latter was saturated at carbons 3 and 4 of the quinoline derivative, whereas pseudobactin is unsaturated at these positions. A mechanism is proposed for the observed conversion of pseudobactin A into pseudobactin in aqueous solution.

When cultured in iron-limiting, complex media, plant growth promoting *Pseudomonas* B10 produces the yellow-green, fluorescent siderophore (microbial iron transport agent) pseudobactin (Kloepper et al., 1980), whose molecular structure is described in the preceding paper in this issue (Teintze et al., 1981). We report here the isolation and structural characterization of yet another siderophore, pseudobactin A, from *Pseudomonas* B10. We also propose a rationale for the observed chemical conversion of pseudobactin A into pseudobactin.

Experimental Procedures

Siderophores. Ferric pseudobactin and pseudobactin were isolated from *Pseudomonas* B10 and purified as described previously (Teintze et al., 1981).

Ferric pseudobactin A and pseudobactin A were obtained from *Pseudomonas* B10 in an analogous fashion with the following modifications. *Pseudomonas* B10 was propagated in the aforementioned minimal medium except that the proteose peptone no. 3 was omitted. This medium is hereby referred to as the chemically defined, glycerol-based minimal medium. The cultures were harvested after 2–3 days. The CM-Sephadex C-25 column chromatography yielded a small red-brown band, which eluted ahead of a purple band consisting of ferric pseudobactin A, followed by a red-brown band containing ferric pseudobactin. The latter two bands overlapped. Ferric pseudobactin A was purified by Bio-Gel P-2 column chromatography as described in the preceding paper in this issue. The yield was typically 25–50 mg/Liter of culture supernatant fluids but varied considerably from run to run. The extinction coefficient of ferric pseudobactin A was obtained as described previously (Teintze et al., 1981).

Pseudobactin A was obtained by deferration of ferric pseudobactin A with 8-hydroxyquinoline according to an earlier procedure (Teintze et al., 1981). Fractions from the Bio-Gel P-2 column chromatography were assayed for iron-binding activity with $Fe(ClO_4)_3 \cdot xH_2O$ as described earlier except that the absorbance of the supernatant fluids at 533 nm was measured. The colorless, nonfluorescent, iron-binding band was concentrated to dryness in vacuo.

Pseudobactin and pseudobactin A were converted into their chloride salts by passing an aqueous solution through a short column containing DEAE-Sephadex A-25, chloride form, equilibrated in water. Both compounds were stored at −70 °C under high vacuum.

Chromatography. Thin-layer chromatography (TLC)[1] was performed as described in the preceding paper in this issue. Ferric pseudobactin A and pseudobactin A were homogeneous by TLC of their solutions.

Time Course of Production of Pseudobactin and Pseudobactin A. Siderophore production from *Pseudomonas* B10 was examined in detail in the chemically defined, glycerol-based minimal medium and in the same medium supplemented with 4 g of deferrated proteose peptone no. 3 per L. *Pseudomonas* B10 was propagated in King's medium B (KB) as described in the preceding paper in this issue. Approximately two drops each were transferred to 2.5 mL of minimal medium with and without proteose peptone no. 3, and these cultures were shaken

† From the Department of Chemistry, University of California at San Diego, La Jolla, California 92093. *Received March 24, 1981.* This work was supported in part by grants from the U.S. Public Health Service (AI 14084) and from the National Science Foundation (CHE-7916324) to the Southern California Regional NMR Facility.

[1] Abbreviations used: NMR, nuclear magnetic resonance; CD, circular dichroism; TLC, thin-layer chromatography; DSS, 3-(trimethylsilyl)propanesulfonic acid, sodium salt; Me_4Si, tetramethylsilane; Me_2SO, dimethyl sulfoxide; β-OH-Asp, β-hydroxyaspartic acid; KB, King's medium B; EDDA, ethylenediaminebis(*o*-hydroxyphenylacetic acid).

0006-2960/81/0420-6457$01.25/0